References

[1] Lees, L. and Yang, H., "Rayleigh's problem at low Mach number according to the kinetic theory of gases," J. Math. Phys. **35**, 195–235 (October 1956).

[2] Grad, H., "On the kinetic theory of rarefied gases," Communs. Pure Appl. Math. **2**, 331–407 (1949).

[3] Lees, L., "A kinetic description of rarefied gas flows," Guggenheim Aeronaut. Lab., Calif. Inst. Tech. Hypersonic Research Project Memo. 51 (December 15, 1959).

[4] Logan, J. G., "On the propagation of transverse disturbances in rarefied-gas flows," J. Aerospace Sci. **29**, 1011–1012 (1962).

[5] Logan, J. G., "Propagation of thermal disturbances in rarefied gas flows," AIAA J. **1**, 699–700 (1963).

Unsymmetrical Buckling of Shallow Spherical Shells

NAI-CHIEN HUANG*

Harvard University, Cambridge, Mass.

THE numerical results for the critical pressure for unsymmetrical buckling of clamped, shallow, spherical shells recently were presented by Weinitschke.[1] The author of the present note independently has obtained results for the same problem which are in striking disagreement with those of Weinitschke. The governing differential equations used agree with those used by Weinitschke. The buckling pressures were calculated numerically. The final results are shown in Fig. 1 together with some available experimental data.[2, 3] The pressure parameter p is defined as the ratio of the external pressure q to the classical buckling pressure q_0 of the complete spherical shell of the same radius of curvature and thickness; n is the number of waves along the circumferential direction appearing in the buckling mode. The disagreement with Weinitschke's results is displayed in Fig. 2, but the reason for this disagreement remains unknown.

According to the author's results, unsymmetrical buckling ($\mathbf{n \neq 0}$) occurs only for $\lambda > 5.5$. For $\lambda < 5.5$, buckling occurs

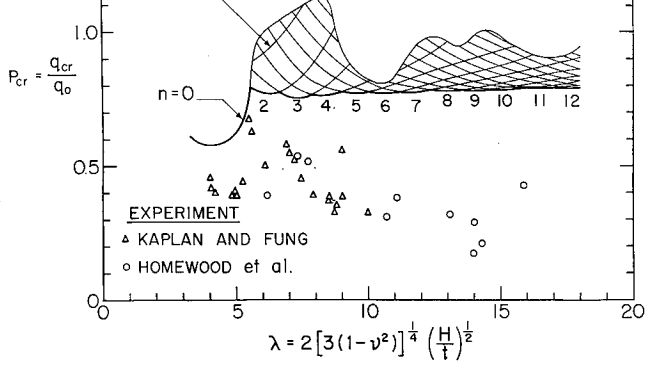

Fig. 1 Calculated buckling pressures of clamped, shallow, spherical shells and experimental results

Received by IAS November 29, 1962. The work was supported by the Office of Naval Research. The author wishes to acknowledge his indebtedness to B. Budiansky, who has given constant encouragement and valuable advice during the whole course of research.

* Research Assistant, Division of Engineering and Applied Physics.

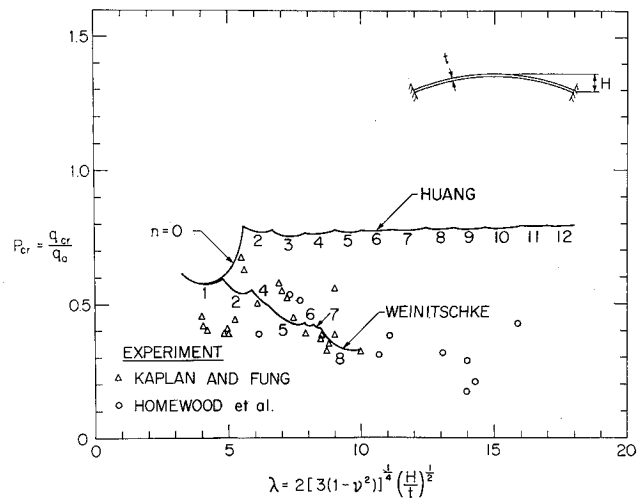

Fig. 2 Calculated buckling pressures vs Weinitschke's results

by axisymmetrical snapping. As λ keeps increasing, the buckling mode shows more and more waves along the circumferential direction and also shows a distinct boundary layer near the edge of the shell along the radial direction when λ is high. An asymptotic value of the buckling pressure is found to be 0.864 when λ approaches infinity and the ratio of n/λ approaches 0.817. Initial imperfections of the shell are presumed to be the source of the discrepancy between theory and experiment.

References

[1] Weinitschke, H. J., "The effect of asymmetric deformations on the buckling of shallow spherical shells," J. Aerospace Sci. **29**, 1141 (1962).

[2] Kaplan, A. and Fung, Y. C., "A nonlinear theory of bending and buckling of thin elastic shallow spherical shells," NACA TN 3212 (August 1954).

[3] Homewood, R. H., Brine, A. C., and Johnson, A. E., Jr., "Experimental investigation of the buckling instability of monocoque shells," Proc. Soc. Exptl. Stress Anal. **18**, 88 (1961).

On Axially Symmetric, Turbulent, Compressible Mixing in the Presence of Initial Boundary Layer

GDALIA KLEINSTEIN*

Polytechnic Institute of Brooklyn, Farmingdale, N. Y.

RECENT experimental results[1] have shown that the mixing of heterogeneous gases having an initial velocity ratio close to unity occurs faster than is predicted by classical eddy-viscosity theory. The theoretical analysis of two uniform streams of different gases but of nearly equal velocity, performed with the usual assumptions for eddy viscosity and Prandtl number equal to a constant,[2] shows that mixing will take place very slowly, i.e., at the rate corresponding to laminar diffusion. It has been suggested that the difference

Received by IAS November 29, 1962. This research was carried out under Contract No. AF 33(616)-7661, administered by the Aeronautical Research Laboratories, Office of Aerospace Research, U. S. Air Force, and is partially supported by the Ballistic Systems Division.

* Research Associate.

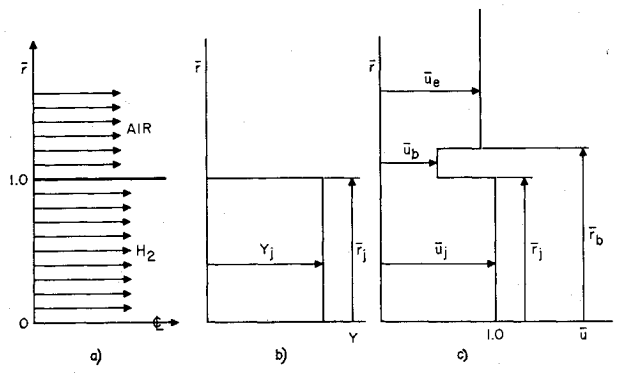

Fig. 1 a) Hydrogen-into-air injection at $u_e/u_j \sim 1$; b) mass concentration, initial profile; c) equivalent velocity, initial profile

between analysis and experiment could be attributed to the presence of a boundary layer in the experiments. It is the purpose of this note to show that the use of the classical eddy-viscosity law, admitting the existence of a boundary layer, is not sufficient to explain the rapid mixing that is observed physically. Instead, it is shown that rapid mixing can be explained on the basis of a different eddy-viscosity law, as was suggested in Ref. 1. These conclusions are obtained through application of the analysis presented briefly below. This work uses the method developed in Ref. 3.

Consider the mixing of two streams of hydrogen and air, as shown in Fig. 1a, with distributions of concentration as shown in Fig. 1b and velocity profiles as shown in Fig. 1c. The velocity profile chosen is such that its momentum and displacement thicknesses are the same as the physical boundary layer. The eddy viscosity is considered to be a function of x only.

The conservation equations for axially symmetric flow with zero pressure gradient, as shown in Refs. 1–4, may be written as

$$\partial P_k/\partial\xi = (1/\psi)(\partial/\partial\psi)[\psi(\partial P_k/\partial\psi)] \tag{1}$$

where P_k can be taken as any one of the following quantities: velocity, stagnation enthalpy, or concentration. The solution of this equation subject to a step-type initial profile, a typical example of which is shown in Fig. 2, namely,

$$\begin{aligned} P_k &= P_{k_m} - P_{k_e} && 0 < \psi < \psi_m \\ &= 0 && \psi_m < \psi \end{aligned} \tag{2}$$

has the form

$$P = \frac{P - P_{k_e}}{P_{k_m} - P_{k_e}} = \frac{1}{2\xi}\exp\left(-\frac{\psi^2}{4\xi}\right) \times \int_0^{\psi_m} \exp\left(-\frac{\psi'^2}{4\xi}\right) I_0\left(\frac{\psi\psi'}{2\xi}\right)\psi' d\psi' \tag{3}$$

The values of the P function are tabulated in Ref. 5 in terms of the independent variables $\psi_m/(2\xi)^{1/2}$ and $\psi/(2\xi)^{1/2}$ as

$$P\left[\frac{\psi_m}{(2\xi)^{1/2}}, \frac{\psi}{(2\xi)^{1/2}}\right] = P\left[\frac{\psi_m}{(2\xi)^{1/2}}, \frac{0}{(2\xi)^{1/2}}\right] \times P^*\left[\frac{\psi_m}{(2\xi)^{1/2}}, \frac{\psi}{(2\xi)^{1/2}}\right] \tag{4a}$$

where

$$P\left[\frac{\psi_m}{(2\xi)^{1/2}}, \frac{0}{(2\xi)^{1/2}}\right] = 1 - \exp\left(-\frac{\psi_m^2}{4\xi}\right) \tag{4b}$$

The inversion to physical coordinates is obtained from the definitions

$$\bar{r}^2 = \int_0^{\psi} \frac{\psi d\psi}{\bar{\rho}\bar{u}} \tag{5}$$

and

$$\xi = \int_0^x 2\bar{\rho}\bar{\epsilon}d\bar{x} \tag{6}$$

where $\bar{\rho}\bar{\epsilon}$ is assumed to be a function of $\bar{x}$ only.

It is possible to superimpose solutions, because of the linear nature of the equations in the ξ-ψ plane. Therefore, the velocity profile of Fig. 1c in the ψ coordinates can be constructed by adding the two profiles u_1 and u_2, as is shown in Fig. 3. The solution for the u_3 profile, in terms of the P function, is given as follows:

$$\bar{u} = \bar{u}_e + (\bar{u}_j - \bar{u}_b)P_1\left[\frac{\psi_j}{(2\xi)^{1/2}}, \frac{\psi}{(2\xi)^{1/2}}\right] + (\bar{u}_b - \bar{u}_e)P_2\left[\frac{\psi_b}{(2\xi)^{1/2}}, \frac{\psi}{(2\xi)^{1/2}}\right] \tag{7}$$

for the velocity, and

$$Y = P_1\left[\frac{\psi_j}{(2\xi)^{1/2}}, \frac{\psi}{(2\xi)^{1/2}}\right] \tag{8}$$

for the concentration.

The values of $\bar{u}_b$ and ψ_b are determined completely by the momentum and displacement thicknesses of the original profile. The radial distributions of velocity, concentration, etc., can be obtained without specifying a particular viscosity law. These distributions are presented in Fig. 4 via application of Eqs. (5–8). The boundary layer data and initial profiles used to obtain the results of Fig. 4 correspond to the values measured experimentally by L. J. Alpinieri in tests of hydrogen-air mixing at the Polytechnic Institute of Brooklyn Aerodynamics Laboratory in Freeport, N. Y. It can be noted (Fig. 4) that the velocity profile decays gradually to a quasi-uniform profile, and the value of the concentration at the center line decreases from 100% at $\xi = 0$ to 51% at $\xi = 0.694$ and 7% at $\xi = 6.25$.

Using the classical expression for the dynamic viscosity coefficient,[1]

$$\overline{\rho\epsilon} = kb_{1/2}\rho_e(u_{\max} - u_{\min}) \tag{9}$$

it is found that $\xi = 6.25$ corresponds to about 300 radii of the initial hydrogen stream. The experimental results obtained

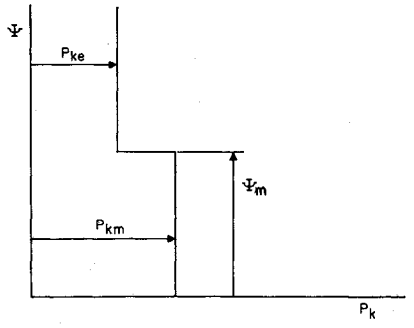

Fig. 2 Step-type initial profile in the ψ coordinate

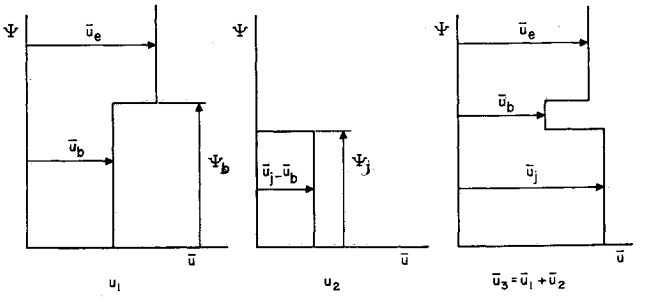

Fig. 3 Superposition in the ξ-ψ plane

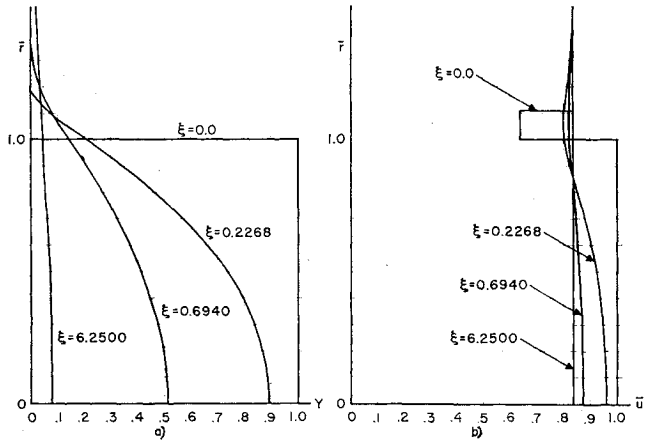

Fig. 4 a) Radial mass concentration; b) radial velocity distribution

by Alpinieri indicate that $\xi = 6.25$ corresponds to about 15 radii, and, consequently, it can be inferred that the classical eddy-viscosity law is not valid. If, on the other hand, the dynamic viscosity coefficient, as suggested by Ferri,[1, 3]

is used,

$$\overline{\rho\epsilon} = kb_{1/2}[(\rho u)_{\max} - (\rho u)_{\min}] \tag{10}$$

$\xi = 6.25$ corresponds now to about 15 radii, which is in agreement with the experimental results. Hence, it appears that the viscosity law described by Eq. (10) is a better formulation for describing the physical phenomena.

References

[1] Ferri, A., Libby, P. A., and Zakkay, V., "Theoretical and experimental investigation of supersonic combustion," Third Internat. Council Aeronaut. Sci. Congress, Stockholm, Sweden (August 27–31, 1962).

[2] Libby, P. A., "Theoretical analysis of turbulent mixing of reactive gases with application to supersonic combustion of hydrogen," ARS J. **32,** 388–396 (1962).

[3] Kleinstein, G., "Axially symmetric mixing in laminar and turbulent compressible flow," Polytechnic Inst. Brooklyn, Ph.D. thesis, PIBAL Rept. 756 (to be published).

[4] Kleinstein, G., "An approximate solution for the axisymmetric jet of a laminar compressible fluid," Polytechnic Inst. Brooklyn, PIBAL Rept. 648, ARL 51 (April 1961); also Quart. Appl. Math. **XX,** 49–54 (1962).

[5] Masters, J. I., "Some applications in physics of the *P*-function," J. Chem. Phys. **23,** 1865–1874 (1955).

Minimizing Weight Penalty for VTOL Performance

B. Saelman*
Lockheed California Company, Burbank, Calif.

GENERALLY, for a given mission, in comparing VTOL aircraft with conventional aircraft, the weight increment in the powerplant, rotor groups, and required fuel associated with lifting systems will be offset partially by reduced weight of landing gears, wing, and possibly the tail. The wing of the VTOL machine might be smaller in some instances, since its geometry is no longer dependent on conventional take-off and landing; the landing gear need not be designed for high-speed rolling take-offs and landings, and the tail need not be sized by take-off and landing requirements or high-speed requirements. To formulate the problem mathematically, proceed from the growth factor concept:

$$\partial W_G/\partial W_F = K \tag{1}$$

The fixed weight includes payload, crew, crew provisions, passengers and provisions, and all other weights that are not directly dependent upon airplane size. The growth factor thus is defined as the total gross weight increment required to accommodate a unit increment of fixed weight or, more generally, the total gross-weight increment corresponding to a unit initial-weight increment of any nature. Although the growth factor expressed by Eq. (1) generally is not constant with gross-weight variations, since it could reduce, for example, with increased structural efficiency as size increases, it will be assumed to be constant for this discussion. Under this assumption, one can write

$$\frac{W_{F_1}}{W_{G_1}} = \frac{W_{F_1} + \Delta W_E + \Delta W_{\text{FLAPS}} + W_R + \Delta W_{\text{FUEL}} - \Delta W_W - \Delta W_T - \Delta W_{LG}}{W_{G_2}} \tag{2}$$

and

$$R = \frac{W_{G_2}}{W_{G_1}} = \frac{\frac{W_{F_1}}{W_{G_1}} + \frac{\Delta W_E}{W_{G_1}} + \frac{\Delta W_{\text{FLAPS}}}{W_{G_1}} + \frac{W_R}{W_{G_1}} + \frac{\Delta W_{\text{FUEL}}}{W_{G_1}} - \frac{\Delta W_W}{W_{G_1}} - \frac{\Delta W_T}{W_{G_1}} - \frac{\Delta W_{LG}}{W_{G_1}}}{W_{F_1}/W_{G_1}} \tag{3}$$

The gross-weight increment for VTOL operation will be minimized when the ratio given by Eq. (3) has its least value. With W_{G_1} fixed, this can be achieved by minimizing W_{G_2}. The ratio R is a minimum when

$$\frac{dR}{dW_{G_1}} = \frac{1}{c}\sum \frac{d(W_i/W_{G_1})}{dW_{G_1}} = 0 \tag{4}$$

From Eq. (3), R vs W_{G_1} can be plotted and the minimum value of R and the corresponding value of W_{G_1} obtained. However, this procedure implies that the optimum gross weight for conventional performance first must be selected and then the payload matched to this gross weight; this is the converse of the usual procedure. However, it still may indicate one possible optimum design point.

Another approach is to require high performance for the conventional aircraft, such as high speed, operating altitude, rate of climb, etc., so that the powerplant size and weight differential between the conventional and VTOL aircraft are minimized.

The gross-weight ratio R can vary from about 1.1 for a supersonic transport to about 2.0 for a modern fighter. The reason that the fighter gross-weight ratio is so high is that the weight increments in the powerplant and fuel required for VTOL performance are not offset significantly by reductions in other components. Thus, for a VTOL fighter using lift engines, the gross-weight increment could be minimized by reducing the specific weight and specific fuel consumption of the engines.

It is obvious from Eq. (3) that the VTOL weight increment reduces with the growth factor. Reduction in growth factor can be accomplished by the many weight-reduction devices that have been discussed. It is interesting to note that for some engines the specific weight will increase and the specific fuel consumption will decrease with size or thrust in some ranges, indicating that this is an area for optimization.

Received by IAS November 26, 1962.

* Design Specialist.